

Study of Multiple Wake Vortex System Behind Aircraft Near Ground Proximity using Prandtl-Lifting Line Theory

S.Paramasivam*, C.L.Poh* and J.U.Schluter **

Corresponding author: mlpchua@ntu.edu.sg

* Nanyang Technological University, Singapore

** Deakin University, Australia

Abstract: In this research, a simplified method using Prandtl-Lifting line theory is proposed to model the multiple wake-vortex system shed behind an aircraft in various high-lift lift configurations. It is proven that the spanwise lift distribution has a great effect on the initial structure, strength and number of vortices formed downstream and their evolution. Further, a particular combination of strength and position of flap vortices are found to effectively enhance the secondary vortex formation in the presence of crosswind. This is evident from the plots of Modified landing configuration which has lowest circulation of all configurations. Hence, this proposed method is also helpful in finding out the optimum lift distribution that alleviates the wake-vortex hazard in shorter duration.

Keywords: Wake-vortex modeling, LES, B747, Span-loading effect, Prandtl-lifting line theory, flap vortex.

1 Introduction

Vortical structures are fascinating flow physics phenomena as it involves a complex time-dependent behavior and intensely high tangential velocities. One such popular vortical flows that is being studied over decades is wake-vortices. They are by-products of lift generation in an aircraft [1]. A wide range of length and time scale are involved in the flow field. The initial condition of the vortices depends on the weight, wing span, speed and configuration of the high-lift devices of the aircraft. Their transport and decay are highly influenced by the ambient atmospheric conditions like crosswind [2], turbulence intensity [3] and Atmospheric stratification [4].

When the airplane is in ground proximity i.e., about one wing span height from ground, the vortices can no longer move downwards due to the presence of boundary layer. The trailing vortices are forced to bounce back and so the effective downwash velocity reduces. The effective angle of attack is higher, and the lift produced is comparatively higher. This is called *in-ground effect*. Further, when the vortices come in close contact with the ground, there is an induced flow over the surface with an opposite sign of vorticity. The adverse pressure gradient, experienced by this induced flow, is strong enough to cause flow separation forming a separation bubble. Secondary vortices are formed from these separation regions. They detach from the ground and interact with the primary vortices leading to rapid decay of the strength of the primary vortices [5-9]. The in-ground effect is particularly a problem when an aircraft is landing/taking-off in an airport. The vortex pair will remain in the runway for a longer time which makes it necessary to have a separation between two landing/taking-off aircrafts.

As the modern aircrafts becomes heavier with more passenger capacity, the holding capacity of the airport is hindered by the imposed wake turbulence separation standard for heavy aircraft category. For almost four decades, there are two types of research conducted in the field of wake-

vortices, one is to understand the vortical structures better and the other is to alleviate the strength of the vortices artificially. In this paper, focus will be given to the numerical tools used to study the wake-pattern. In general, there are four phases of wake-vortex evolution as follows: wake-formation zone, stable wake zone, unstable wake-zone and wake breakdown zone [10]. Most of the researches have treated the vortex roll-up process, development and decay as separate problems. The vortices formed are at different altitudes from ground and at different ages when an aircraft approaches until it touches down. Many researches focus on simulating the wake-vortices as a pair of counter rotating vortex filament initialized using various available vortex models [11]. This may help in understanding the general vortex behavior in ground proximity, but the appropriate method is to consider the phases of the aircraft if the results should be of practical significance. One such successful method of considering different phases of the aircraft is the use of Hybrid LES/RANS method by DLR [7]. RANS is used for calculating the flow field around the landing aircraft in high-lift configuration and LES for far-field evolution of the shed velocity field. As of today, this is most known method for simulating the vortices from roll-up to decay, through all phases of the landing flight.

To simulate a vortex from roll-up to decay, it is important to know the effect of spanwise lift distribution over wing on the formation of wake-vortices. Its significance can be found from the research work done by Brown [12] and Rossow [13-19]. The research by Brown shows that the trailing vortices formed due to a parabolic and elliptic wing loading are different from each other. Rossow conducted extensive experimental research on influence of span loading in different lifting configurations on the wake vortices. Most of the experiments are conducted on the Boeing 747 scaled down model in water-tunnel facility and some are conducted as real-time measurements. While it is clearly evident from his works that the span loading plays a major role, there are still gaps in understanding the flow phenomena. In this paper, the multiple vortex pair system shed by different aircraft configurations are studied and their vortex interactions are explained in detail.

2 Methodology

In this research, a new simulation package, a set of FORTRAN codes developed by Charles Pierce [20]. Pierce has used the LES technique with the dynamic approach of co-efficient calculation for solving the non-linear Navier-Stokes' equation. The computational grid used defines filtering implicitly. The filtered momentum equation is solved using iterative Semi-implicit scheme in time. Finite difference method is used to calculate the spatial and time derivatives. Staggered grid discretization for velocity is implemented in spatial and temporal directions. The code is modified and already validated for the wake-vortex problem with experimental results [21]. Lamb-Oseen vortex model [22] is used to model the multiple vortices shed from the wing based on the spanwise circulation distribution gradient.

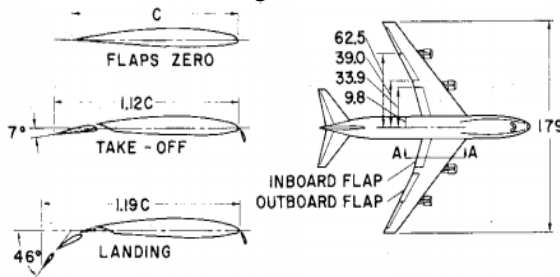


Figure 1a: Specifications of B747 [23]

Parameters of B747	Landing	Take-off
Initial circulation (m ² /s)	554.6	633.3
Aircraft speed (m/s)	80	97.3
Characteristic velocity scale (m/s)	1.75	1.99
Characteristic time scale	29 s	25.4 s
Wing span, b ₀	64.4 m	

According to Prandtl-lifting line theory, for any change in the lift distribution over a wing segment, a vortex is shed in the downstream with a circulation strength proportional to that of the lift. Hence, the spanwise circulation distribution is calculated using the formula,

$$\Gamma(y) = \frac{1}{2} V_{\infty} c(y) c_l(y)$$

The spanwise lift distribution of B747 aircraft is considered to prove the working of this simplified numerical model for different aircraft configuration (figure 1a, 1b and 1c) [14].

The B747 configurations considered for the study are mentioned in the table below,

Case 1	A pair of fully developed vortices.
Case 2	Take – off configuration
Case 3	Landing configuration (LDG) Inboard (IB) flap = 46° Outboard (OB) flap = 46°
Case 4	Modified Landing configuration -1 (MLDG-1) Inboard (IB) flap = 46° Outboard (OB) flap = 0°
Case 5	Modified Landing configuration -1 (MLDG-2) Inboard (IB) flap = 0° Outboard (OB) flap = 46°

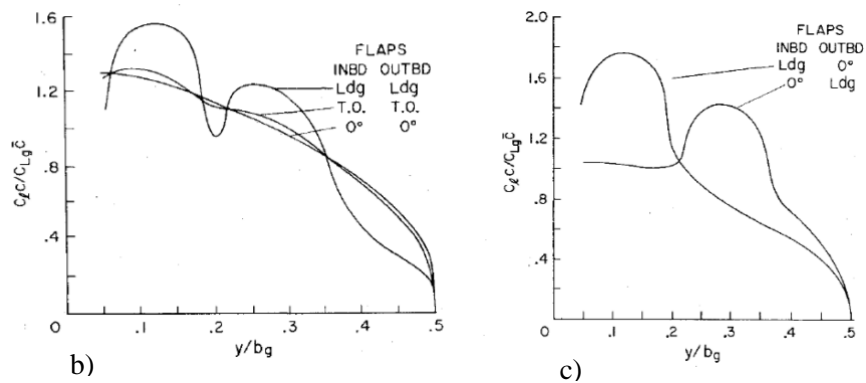


Figure 1. b) and c) Spanwise-lift distribution for different configuration of B747 [14].

The dimension of the computational domain is $8b_0 \times 5b_0 \times 8b_0$. In the flight path direction and its perpendicular direction, a periodic boundary condition is imposed. No slip condition is set at $z=0$ and $z=z_{max}$. Even though the top plane is defined as no-slip condition it is at a considerably higher altitude so that their boundary layer does not affect the flow characteristics. By performing grid independency study, 33.3 million node points are selected to be optimum for this problem [23]. There is a background crosswind flow of 1.72m/s. For simplicity, the atmospheric turbulence intensity is neglected in the study.

3 Results and Discussion

3.1 Circulation characteristics

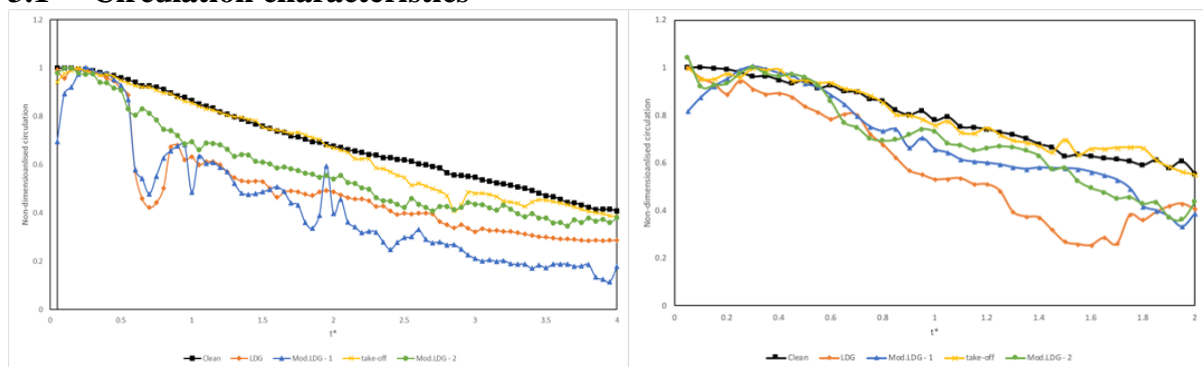


Figure 2: Evolution of circulation for upwind and downwind vortex

The circulation characteristics of the upwind and downwind vortices for different configurations are presented in fig.2. The primary vortices induce a flow over the ground which creates a boundary layer with vorticity sign opposite to that of each of the primary vortices. In the presence of crosswind, there will be a boundary layer separation near ground leading to the formation of secondary vortices

especially around downwind vortex. These secondary vortices enhance the dissipation of primary vortices [6]. Downwind vortex is of less concern since they exit the runway in a very short time. Hence, in this study, only the upwind vortex and their flap vortices are given higher importance. The evolution of circulation for take-off is similar to that of elliptical wing loading. As illustrated in fig.3a, 3b, the vortex evolves to a pair of counter rotating vortices.

For all the three landing configurations, the evolution of circulation follows the *two-phase decay* model. There is a short phase of diffusion until $t^* = 0.5$ and then there is a rapid-decay phase. It must be noted that the circulation of MLDG-2 is higher than LDG which is higher than that of MLDG-1, at any given time in the rapid decay phase. This is due to the strength, number and degree of interaction of secondary vortices formed with the primary vortex. The sudden drops in the circulation plot for case 3 and 4 is due to the interaction of flap vortices and primary vortex at the mid-plane for which the data is plotted. The modified landing configuration-1 results in the lowest circulation strength than any other configurations. This is in correlation with the experimental results obtained [14]. Detailed explanation of the interaction between flap vortices different landing configuration is given in the subsection 3.2.

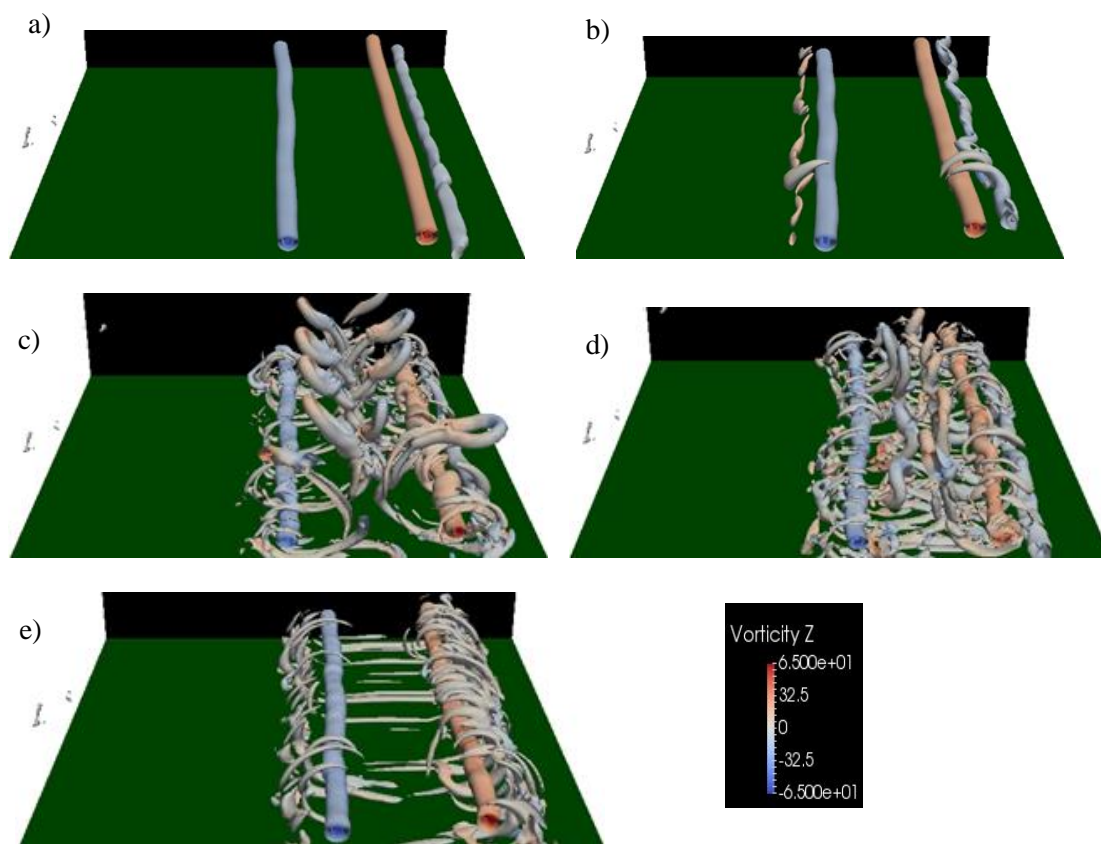


Figure 3: Tangential Vorticity isosurfaces for different configurations at $t^* = 1.65$. a) Single pair vortex system, b) Take-off, c) LDG, d) MLDG – 1, e) MLDG – 2

3.2 Comparison of Different Landing Configurations

For every change in the lift distribution, there will be a vortex shed downstream. Hence, the strength of the vortices is proportional to the gradient of the lift distribution. While the tip vortex and OB flap vortices are of same sign, the IB flap vortices are in opposite sign to them in all three cases (figure 4). For LDG configuration, there are three pair vortices shed from the wing-tip, IB and OB flap. The tip vortices are of higher strength compared to the OB flap vortices. For the MLDG-1 configuration, the wing tip and OB flap vortices are of comparable strengths and more diffused. Also, this diffused vortex structure enables the primary vortices to be closer to the IB flap vortices resulting in enhanced interaction. For the case of MLDG-2 configuration, the OB flap is retracted and so, only the wing tip

vortices and IB flap vortices are prominently seen in the flow field. The IB flap vortices have lower strength compared to other cases. It can be seen from all three plots that the initial vortices are more diffused and are completely different in structure compared to the fully developed two pair vortex system.

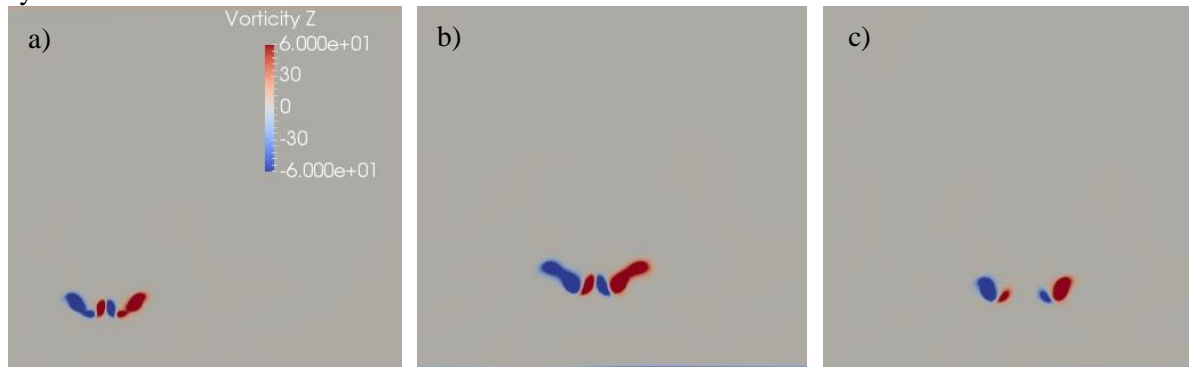


Figure 4: Tangential Vorticity contour plot for different configurations at $t^* = 0.05$.

a) LDG, b) MLDG - 1, c) MLDG - 2

From fig.5a, 5b and 5c, it is evident that the secondary vortices formed are also different for each landing cases. At the onset of rapid-decay phase, in LDG configuration, the secondary vortices are initially of higher strength due to the presence of stronger flap vortices. For MLDG-1 configuration, the secondary vortices formed may not be of a strength as high as that of LDG, but the degree of interaction is higher. In the case of MLDG-2, the onset of secondary vortices is earlier but the strength and the interaction with primary vortices are comparatively lesser than the other two configurations. At later time steps, the secondary vortices interaction and strength is highest in the case of MLDG-1 which explains the lowest circulation value (figure 6). The omega-loop structured formed around each of the primary vortices are alternative. These vortices are to be studied further to have clear understanding on how to leverage these vortices to enhance the dissipation.

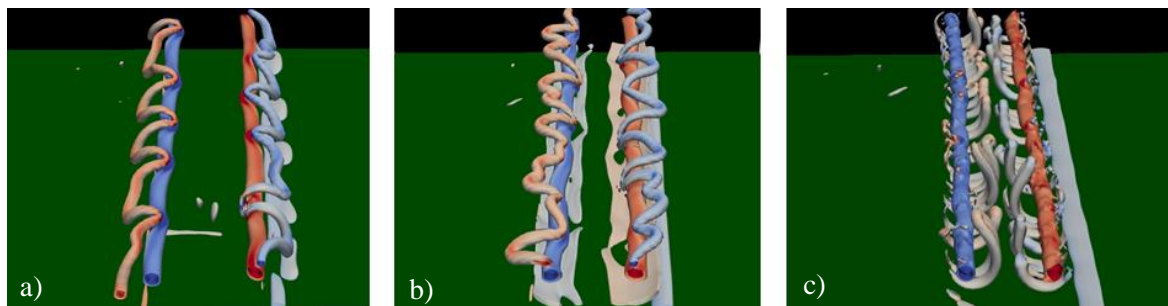


Figure 5: Tangential Vorticity isosurfaces for different configurations at $t^* = 0.65$.

a) LDG, b) MLDG - 1, c) MLDG - 2

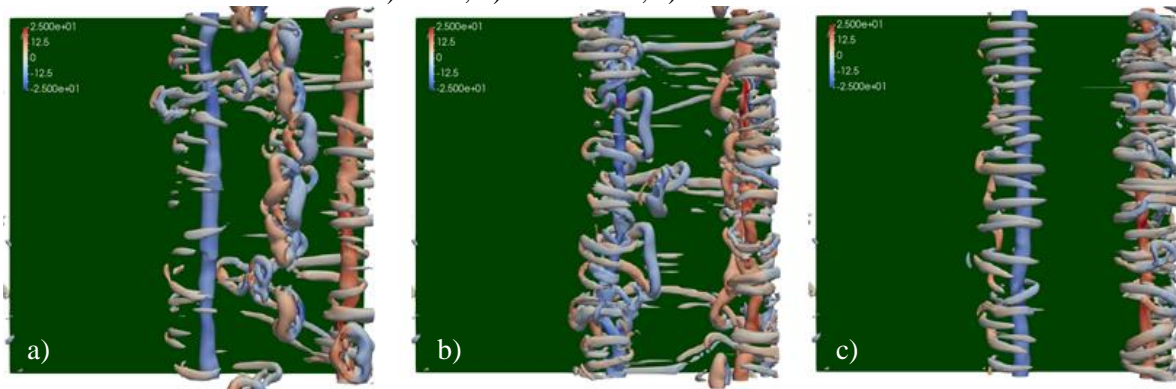


Figure 6: Tangential Vorticity isosurfaces for different configurations at $t^* = 2.5$.

a) LDG, b) MLDG - 1, c) MLDG - 2

MLDG-1 configurations are proven to be most effective in alleviating the primary vortices strength. At first instance, it will be expected that the LDG configuration is highly effective, but the secondary vortices formed are transported away from the primary vortices with time (figure 7), resulting in vortex ring formation (figure 8). This reduces the interaction between the primary and secondary vortices.

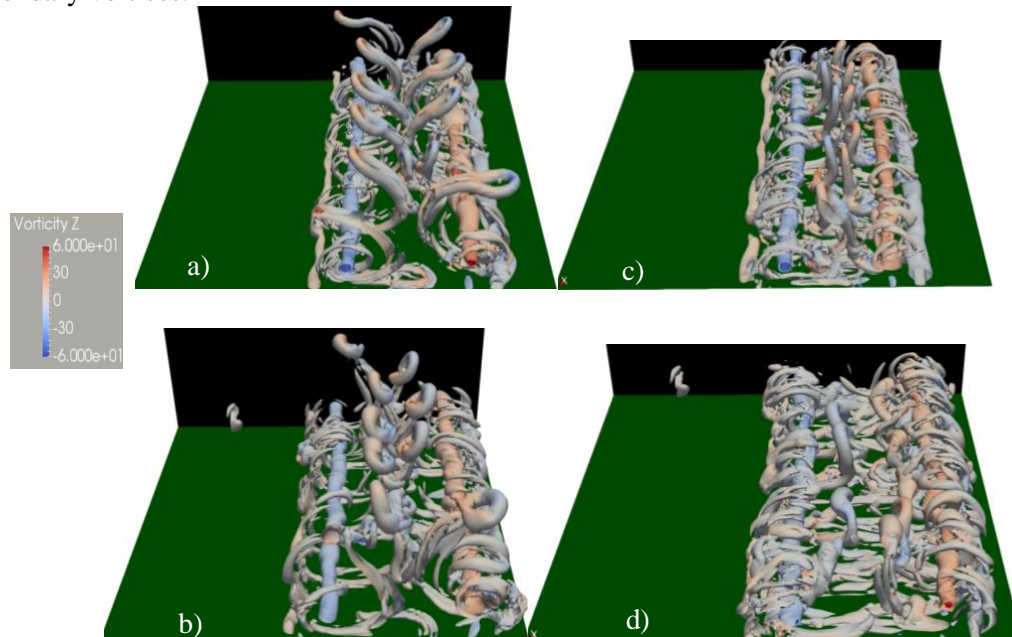


Figure 7: Tangential Vorticity isosurfaces for different configurations at $t^* = 2.5$.
a) $t^* = 1.5$ (LDG) , b) $t^* = 2.0$ (LDG), c) $t^* = 1.5$ (MLDG-1) , d) $t^* = 2.0$ (MLDG-1),

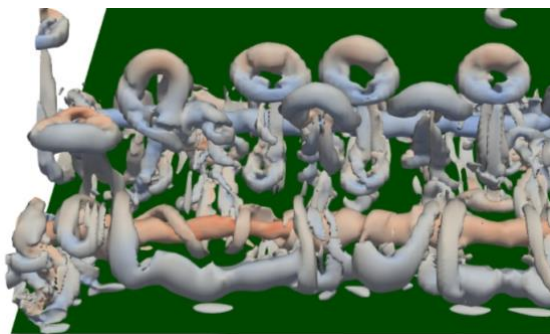


Figure 8: Vortex ring formation in LDG configuration at $t^* = 2.0$.

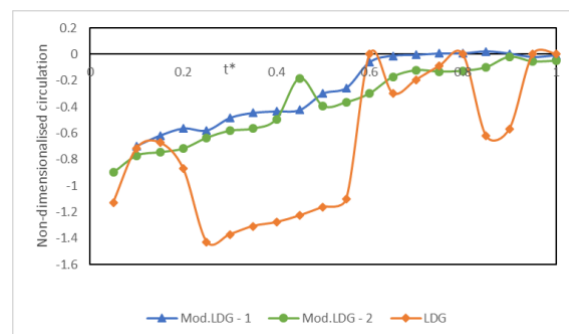


Figure 9: Circulation strength of IB flap vortices around upwind vortex for different landing configuration.

3.3 Flap Vortices

In this subsection, the flap vortices are investigated in detail. It is a common misconception that the influence of flap vortices is negligible as it merges with the primary vortices within few seconds. But the flap vortices shed from wings plays a crucial role in the onset of secondary vortices. The position and strength of the IB flap vortices affects the flow over the ground induced the primary vortices which in turn influences the formation of secondary vortices. Since the induced boundary layer vorticity and flap vortex are of same sign, the instability in IB flap vortex enhances the secondary vortex formation. But the effectiveness of IB flap vortices depends highly on its position and strength with respect to the primary vortex. For example, the circulation strength of the IB flap vortices is highest for LDG, then for MLDG-1 and then for MLDG-2. But in LDG configuration case, the flap vortices are between primary vortices and ground between $t^*=0.3 - 0.5$ with a highest negative circulation. This reduces the induced flow over the ground resulting in the delayed secondary vortices formation as shown in fig.10.

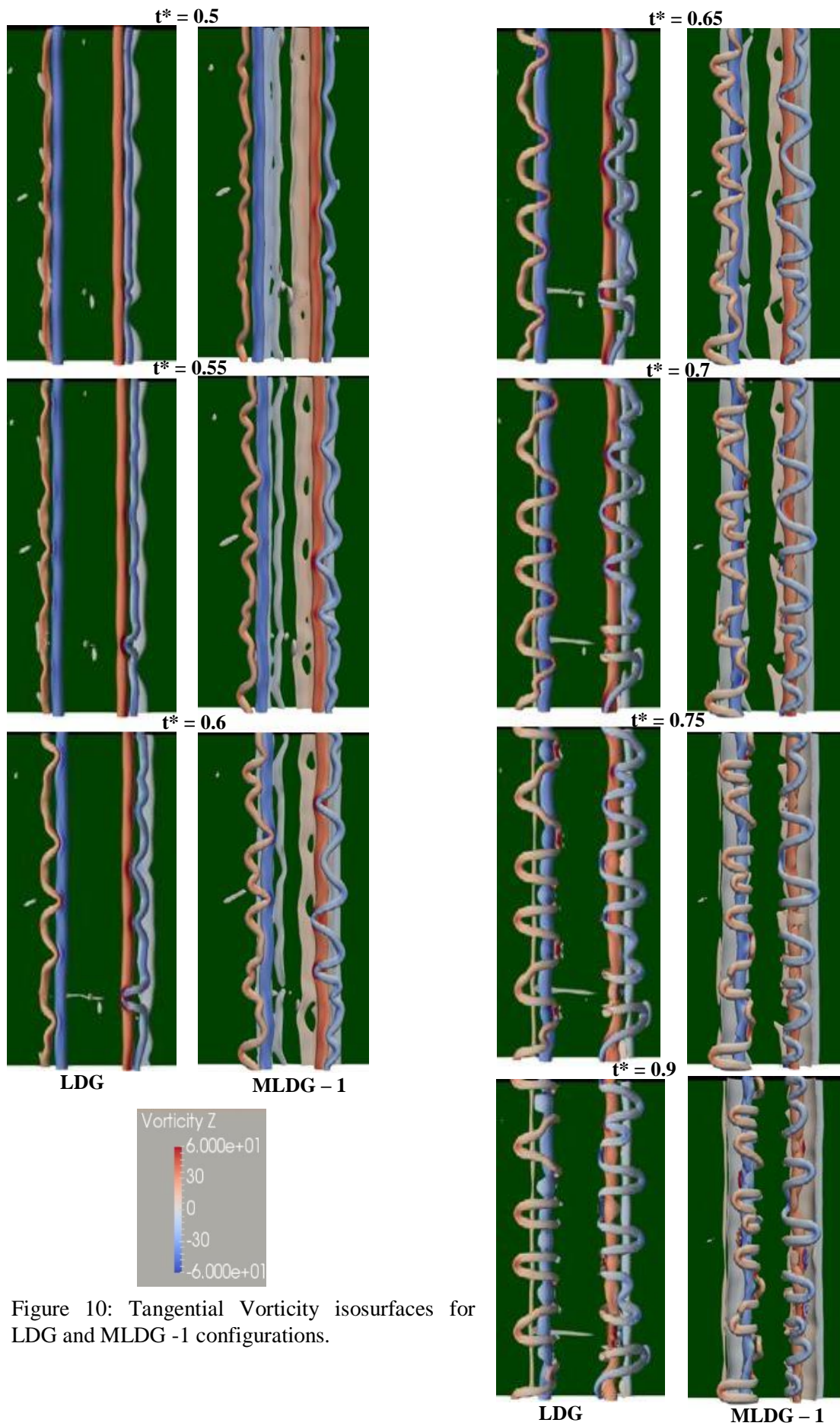


Figure 10: Tangential Vorticity isosurfaces for LDG and MLDG -1 configurations.

4 Conclusion and Future Work

The importance of wake-vortex roll-up phase and their dependency on spanwise-lift distribution is addressed in this paper. The proposed numerical method is proven to be effective, simple and time efficient substitute for studying the influence of span loading on wake vortices. The evolution of wake-vortices for take-off and two pair vortex system, is almost identical. The LDG configuration results in a stronger wing-tip vortex and IB flap vortex. This flap vortex, in general, enhances the secondary vortices formation but the effectiveness is limited by the position and strength of the IB vortex. In the case of MLDG-1, the tip vortices and IB flap vortices are dominant in the flow. The onset of secondary vortices is earlier and also their degree of interaction with the primary vortex is higher for this configuration. Thus, it results in a lowest circulation value at all time-steps compared to other landing configurations. MLDG-2 starts off with stronger wing-tip vortices and weaker IB flap vortices. Hence, the secondary vortices formed are also of lesser strength and proven to be ineffective. Future studies will encompass improvement to this method to include vortex ages and end effects. The improved method will then be used to manipulate the lift distribution and alleviate the wake-vortices in ground proximity artificially.

References

- [1] J. Anderson. *Fundamentals of Aerodynamics* (McGraw-Hill Series in Aeronautical and Aerospace Engineering), 2010.
- [2] K. Dengler, F. Holzäpfel, T. Gerz, A. Wiegele, I. De Visscher, G. Winckelmans, L. Bricteux, H. Fischer, J. Konopka. Crosswind thresholds supporting wake-vortex-free corridors for departing aircraft. *Meteorological Applications*, 19:289-301, 2012.
- [3] H. T. Liu. Effects of ambient turbulence on the decay of a trailing vortex wake. *Journal of Aircraft*, 29:255-63, 1992.
- [4] F. Holzäpfel, T. Gerz. Two-dimensional wake vortex physics in the stably stratified atmosphere. *Aerospace science and technology*, 3:261-70, 1999.
- [5] F. Holzäpfel, M. Steen. Aircraft wake-vortex evolution in ground proximity: analysis and parameterization. *AIAA journal*, 45:218-27, 2007.
- [6] Stephan, F. Holzäpfel, T. Misaka. Aircraft wake-vortex decay in ground proximity—physical mechanisms and artificial enhancement. *Journal of Aircraft*, 50:1250-60, 2013.
- [7] Stephan A, Holzäpfel F, Misaka T, Geisler R, Konrath R. Enhancement of aircraft wake vortex decay in ground proximity. *CEAS Aeronautical Journal*, 5:109-25, 2014.
- [8] W. H. David, H. P. Fred. *Wake Vortex Transport in Proximity to the Ground*, 2000.
- [9] F. Proctor, J. Han. Numerical study of wake vortex interaction with the ground using the Terminal Area Simulation System. In *37th Aerospace Sciences Meeting and Exhibit*, p. 754, 1999.
- [10] S. Ginevsky, A. I. Zhelannikov. *Vortex wakes of Aircrafts*. Springer Science & Business Media, 2009.
- [11] T. Gerz, F. Holzäpfel, D. Darracq, A. de Bruin, A. Elsenaar, L. Speijker, M. Harris, M. Vaughan, A. A. Woodfield. Aircraft wake vortices: a position paper. *Wakenet, the european thematic network on wake vortex position paper*, 2001.
- [12] C. E. Brown. Aerodynamics of wake vortices. *AIAA Journal*, 11:531-6, 1973.
- [13] V. J. Rossow. Wake hazard alleviation associated with roll oscillations of wake-generating aircraft. *Journal of Aircraft*, 23:484-91, 1986.
- [14] V. R. Corsiglia, V. J. Rossow, D. L. Ciffone. Experimental study of the effect of span loading on aircraft wakes. *Journal of Aircraft*, 13:968-73, 1976.
- [15] V. R. Corsiglia, R. E. Dunham Jr. Aircraft wake-vortex minimization by use of flaps., 1977
- [16] D. L. Ciffone, K. L. Orloff. Far-field wake-vortex characteristics of wings. *Journal of Aircraft*, 12:64-70, 1975.

- [17] D. C. Burnham, J. N. Hallock, I. H. Tombach, M. R. Brashears, M. R. Barber. Ground-Based Measurements of the Wake Vortex Characteristics of a B-747 Aircraft in Various Configurations. Transportation Systems Center Cambridge Mass, 1978.
- [18] R. A. Jacobsen, B. J. Short. A flight investigation of the wake turbulence alleviation resulting from a flap configuration change on a B-747 aircraft., 1977.
- [19] V. Rossow. Vortex structures and span loadings from alleviated-wake measurements. In 15th Applied Aerodynamics Conference., p. 2262, 1997.
- [20] C. D. Pierce, P. Moin. Progress-variable approach for large-eddy simulation of turbulent combustion. California, USA: stanford university., 2001.
- [21] S. Paramasivam, D. Zhao, M. Skote, J. U. Schluter. Detailed study of effects of crosswind and turbulence intensity on Aircraft wake-vortex in ground proximity. In 34th AIAA Applied Aerodynamics Conference., p.4184, 2016.
- [22] H. Lamb. Hydrodynamics. Cambridge university press. 1932.
- [23] L. Kantha. Decay of aircraft wake vortices under daytime free convective conditions. Journal of Aircraft., 47:2159-64, 2010.
- [24] V. J. Rossow. Lift-generated vortex wakes of subsonic transport aircraft. Progress in Aerospace Sciences., 35:507-660, 1999